

EXPERIMENTAL AND NUMERICAL MODELING OF OUTRIGGER SYSTEMS
OF TALL BUILDING STRUCTURES

BAHRAM MARABI

A thesis submitted in fulfillment of the
requirements for the award of the degree of
Doctor of Philosophy (Civil Engineering)

School of Civil Engineering
Faculty of Engineering
Universiti Teknologi Malaysia

APRIL 2022

ACKNOWLEDGEMENT

Praise Be to Allah S.W.T, the Lord of the World

Foremost, I would like to express my sincere gratitude to my supervisors Assoc. Prof. Ts. Dr. Sophia C. Alih. And Assoc. Prof. Ts. Dr. Mohammadreza Vafaei for the continuous support of my study and research, for her patience, motivation, enthusiasm, and immense knowledge. Their guidance helped me in all the time of research and writing of this thesis. I could not have imagined having better advisors and mentors for my study.

My sincere thanks also go to all staff, lectures, and individuals who directly or indirectly support me throughout completing this study. I am deeply thankful to my friends and officemates who always support and motivate me during ups and downs.

ABSTRACT

The tall building's height recently has exceeded a thousand meters. An appropriate lateral load resisting system to drift-control seems necessary. Considering that the lateral deflections play a vital role in selecting the type of tall building structures. Top-drift in tall buildings has not yet been entirely resolved for seismic demands. That is way, utilizing the structural outrigger systems is one of the most efficient structural systems to enhance the structure's lateral stiffness and minimize the top-drift without increasing the building's components sizes and mass it will need. This study aims to specify the lateral resisting responses of conventional structural outrigger models through experimental works. A new type of outrigger model was proposed to compare its effectiveness with the conventional models. Finally, to optimize the parameters affecting the new outrigger model's lateral response is proposed through the Finite Element Method (FEM). A total of eight 3D models including three types of structural core models (no outrigger), two types of single outrigger models, two types of multi outrigger models, and a proposed new outrigger model, were experimented using a quasi-static cyclic test. The models are termed the Core Models (Core-1,2 and 3), Opti-models (1-Out, 2-Out), Conv-models (Cap-Out, 2-Out), new model (Dev-Out) and FE Dev-Out. This research, inspired by the 2D analytical method with an idealized pattern, has been used to advance to 3D experimental modeling to achieve more reliable results. The hysteresis curves have been calculated to obtain the initial lateral stiffness, effective stiffness, ultimate lateral strength, ductility ratio, energy dissipation capacity, and failure mechanism in all experiments through the quasi-static cyclic test models. Results indicated that the outrigger systems' optimal forms failed at the first outrigger's upper level while the conventional forms and core models failed at the base. The 2-Out optimal form up to 140% have higher effective stiffness than 1-Out, and Cap-Out 36% higher than 2-Out conventional form, while the Dev-Out form is 31% higher than the 1-Out Opti model. The Cap-out 6% is higher than the 1-Out Opti form as well. The energy dissipation of the 2-Out conventional form has the highest level by 686.1 kN.mm, while the Dev-Out model has the lowest value by 297.7 kN.mm than other outrigger forms. The 2-Out conventional form by 6.73 is ductile, and the 2-Out Opti model by 3.84 ratios has a second-place than other forms. The proposed new model can increase the effective lateral stiffness by 2.2 times at the develop-outrigger location due to added outer peripheral columns. The FE Dev-Out model to reduce the top-drift was optimized when the outrigger is placed at 0.4H from the top of the model. Also, the base moment was minimized if the outrigger is placed at the mid-height and base position range. In final, the developed 3D method compared to the traditional 2D methods indicated a significant difference in the conventional outrigger forms' performance with optimal forms under lateral loads, stiffness, ductility, and energy dissipation in tall building structures.

ABSTRAK

Ketinggian bangunan pencakar langit akhir-akhir ini telah melebihi seribu meter. Sistem penahan beban sisi yang sesuai untuk kawalan anjakan adalah perlu. Memandangkan pesongan sisi memainkan peranan penting dalam memilih jenis struktur bangunan tinggi, anjakan besar di bangunan tinggi belum dapat diatasi sepenuhnya untuk beban seismik. Oleh yang demikian, penggunaan sistem pencetus struktur adalah salah satu sistem yang paling efisien bagi meningkatkan kekakuan sisi struktur dan meminimumkan anjakan tertinggi tanpa meningkatkan ukuran dan jisim komponen bangunan. Kajian ini bertujuan untuk membandingkan tindak balas sisi sistem pencetus struktur konvensional yang berbeza melalui kerja-kerja eksperimen. Model pencetus jenis baru dicadangkan untuk membandingkan keberkesannya dengan model konvensional melalui eksperimen. Akhirnya, untuk mengoptimumkan parameter yang mempengaruhi tindak balas sisi model pencetus baru dicadangkan melalui kaedah unsur terhingga (FEM). Sebanyak lapan model 3D merangkumi tiga jenis model teras struktur, dua jenis model pencetus tunggal, dua jenis model pencetus pelbagai, dan model pencetus baru yang dicadangkan, dieksperimen menggunakan ujian kitaran kuasi-statik. Models tersebut dinamakan Core Models (Core-1,2 and 3), Opti-models (1-Out, 2-Out), Conv-models (Cap-Out, 2-Out), new model (Dev-Out) and FE Dev-Out. Penyelidikan ini, yang diilhami oleh kaedah analitik 2D dengan corak ideal, telah digunakan untuk dimajukan ke model eksperimen 3D bagi mencapai hasil yang lebih dipercayai. Lengkung histeresis telah dianalisa untuk mendapatkan kekakuan sisi awal, kekakuan berkesan, kekuatan sisi akhir, nisbah kemuluran, kapasiti pelepasan tenaga, dan mekanisma kegagalan dalam semua eksperimen melalui model ujian kitaran kuasi-statik. Hasil menunjukkan bahawa bentuk optimum sistem pencetus telah gagal di bahagian atas pencetus pertama sementara bentuk konvensional dan model teras telah gagal di bahagian asas. Bentuk optimum 2-Out mempunyai kekakuan efektif sehingga 140% lebih tinggi daripada 1-Out, dan Cap-Out 36% lebih tinggi daripada bentuk konvensional 2-Out, sementara bentuk Dev-Out 31% lebih tinggi daripada model 1-Out Opti. Cap-out 6% lebih tinggi daripada bentuk 1-Out Opti juga. Pembebasan tenaga dari bentuk konvensional 2-Out mempunyai tahap tertinggi sebanyak 686.1 kN.mm, sementara model Dev-Out mempunyai nilai terendah sebanyak 297.7 kN.mm daripada bentuk pencetus lain. Bentuk konvensional 2-Out dengan 6.73 adalah mulur, dan model 2-Out Opti dengan nisbah 3.84 mempunyai tempat kedua daripada bentuk lain. Model baru yang dicadangkan dapat meningkatkan kekakuan sisi yang efektif sebanyak 2.2 kali pada lokasi pengembangan-pencetus disebabkan penambahan tiang periferal luar. Model FE Dev-Out untuk mengurangkan anjakan atas akan dioptimumkan apabila pencetus diletakkan pada 0.4H dari bahagian atas model. Juga, momentum asas akan diminimumkan jika pencetus diletakkan pada jarak pertengahan dan kedudukan asas. Kesimpulannya, kaedah 3D yang dibangunkan berbanding dengan kaedah 2D tradisional menunjukkan bahawa terdapat perbezaan yang signifikan dalam prestasi bentuk pencetus konvensional dengan bentuk yang optimum di bawah beban sisi, kekakuan, kemuluran dan pelepasan tenaga dalam struktur bangunan tinggi.

TABLE OF CONTENTS

	TITLE	PAGE
	DECLARATION	iii
	DEDICATION	iv
	ACKNOWLEDGEMENT	v
	ABSTRACT	vi
	ABSTRAK	vi
	TABLE OF CONTENTS	vii
	LIST OF TABLES	xviii
	LIST OF FIGURES	xxi
	LIST OF ABBREVIATIONS	xxxiii
	LIST OF SYMBOLS	xxxiv
	LIST OF APPENDICES	xxxvi
CHAPTER 1	INTRODUCTION	1
1.1	Background of the Study	1
1.2	Statement of the Problem	6
1.3	Objectives of the Study	7
1.4	Scope of the Study	8
1.5	Significance of the Study	10
1.6	Thesis Layout	10
CHAPTER 2	LITERATURE REVIEW	13
2.1	Introduction	13
2.2	Definition of Tall Building	15
2.3	Tall Buildings' Structural Systems	16
2.4	Lateral Load Resisting Systems for RC Tall Buildings	17
2.4.1	Lateral Forces Affecting Tall Buildings	19
	2.4.1.1 Effects of Wind Loads	20
	2.4.1.2 Effects of Earthquake Loads	21
2.5	Design Philosophy of Lateral Loads	21

2.6	The Concept of the Outriggered Structural Systems	23
2.7	Optimum Location, Topology, Constraints, Material, and Stiffness of the Outrigger Systems	24
2.7.1	Design Considerations in Outrigger Systems	25
2.7.1.1	Delay Joint Outrigger Connection	26
2.7.1.2	Adjustable Outrigger Connection	26
2.7.1.3	Cross-Jack System	27
2.7.1.4	Shim-Plate Correction Method	28
2.7.1.5	Retro-Casting Techniques in Outriggers Construction	29
2.7.2	Damped Outrigger System	29
2.7.3	Concrete Outrigger System with Structural Fuse	30
2.8	Analytical Models on Performance of the Outrigger Systems	31
2.8.1	Performance of Outrigger Systems	31
2.8.1.1	Behaviour of Outrigger Systems	32
2.8.1.2	Cap Outrigger System	33
2.9	Calculations of Lateral Deflection	36
2.9.1	Outrigger at the Top $x = 0$ or $Z = L$	37
2.9.1.1	Outrigger at $Z = 0.75L$ or $x = 0.25$	38
2.9.1.2	Outrigger at $Z = 0.5L$ or $x = 0.5$)	41
2.9.1.3	Outrigger at $Z = 0.25L$ or $x = 0.75$	42
2.9.2	Optimisation of Outrigger Structural Systems	43
2.9.2.1	Optimisation of a Single Outrigger System	44
2.9.2.2	Optimisation of Two Outriggers Systems	46
2.9.2.3	Optimisation of N-Outrigger systems	51
2.9.3	Parametric Optimisation of Outrigger Systems	52
2.9.4	Efficiency Outriggered Structural Systems	53
2.9.5	Evaluation of Outriggered Structural Systems	54
2.9.5.1	The Efficiency of Single Outrigger Systems	54
2.9.5.2	The Efficiency of Two-Outrigger Systems	55
2.9.5.3	Optimum Locations of Multi-Outrigger Systems	56

2.10	Numerical Studies on Response of The Outrigger Systems Due to Lateral Loads	61
2.10.1	Design Criteria Tall Buildings Structure	61
2.10.1.1	Assessment of the Outrigger Systems Under Earthquake Hazard Levels	62
2.10.2	Seismic Design Purposes	62
2.10.3	Analysis Procedures of Tall Buildings structure	63
2.10.3.1	Linear Procedures Analysis	63
2.10.3.2	Non-linear Procedures Analysis	67
2.10.4	Control Deflection in Tall Building Using Outrigger Systems	70
2.10.4.1	Optimum location of outrigger	71
2.10.4.2	Secondary Data of Optimum Locations of the Outrigger	75
2.10.5	Finite Element Modelling of the Structure of the Tall Building	78
2.11	Experimental Researches on Performance of the Outrigger Systems	80
2.11.1	Purposes of The Experimental Study	80
2.11.2	The Experimental Studies on the Outrigger Systems	81
2.12	Summary of Literature Reviews	82
CHAPTER 3	METHODOLOGY	85
3.1	Introduction	85
3.2	General Procedures	86
3.3	Flowchart of Methodology	87
3.4	3D Modelling, Configuration and Forms the Sets of the Outriggers	89
3.5	Conducting Experimental Studies	92
3.5.1	Experimental Study	93
3.5.2	Introduction to Experimental Tests Cases under Investigation	96

3.5.3	Materials Used in Fabrication of the Laboratory Models	98
3.5.3.1	Tensile Test to Determine Material Properties	100
3.5.4	Fabrication of the Experimental Models	103
3.5.5	Stiffness Ratio Method (SRM) to Build Down-Scale Experimental Models	105
3.5.6	Specifications Laboratory Models	110
3.5.7	Experimental Testing Procedures	113
3.5.7.1	Quasi-Static Cyclic Test	113
3.5.8	Experimental Testing Framework	114
3.5.8.1	Base Set-up	115
3.5.8.2	Placing of the Models in the Testing Frame	117
3.5.8.3	Test Set-up and Relevant Instruments	119
3.5.9	Instrumentation on Models	124
3.5.9.1	Core Structural Models Instruments	124
3.5.9.2	Single Outrigger Model	125
3.5.9.3	Multi outrigger Models	127
3.5.9.4	Proposed New Outrigger Model	129
3.5.10	Test Procedure	130
3.6	Numerical 3D Finite Element Modelling (FEM) and Analysis (FEA)	132
3.6.1	Introduction to Numerical Study	132
3.6.2	Overview of Modelling by Abaqus/CAE	133
3.6.3	Modelling Procedures within Abaqus/CAE	133
3.6.3.1	Elements	134
3.6.3.2	Mesh Size of Structural Elements to Optimise Model	135
3.6.4	Type of Analysis in Abaqus/CAE	136
3.6.4.1	Static, General Step Procedure	137
3.7	Material Properties Used in Abaqus	137
3.8	Simulation of the Finite Element Models in Abaqus/CAE	138

3.8.1	Finite Element Modelling Connections	140
3.8.2	Definition Types of Boundary Connections	141
3.8.3	Definition of Loading Types	142
	3.8.3.1 Definition of Load for the Numerical Experiments models into Abaqus/CAE	143
3.8.4	Definition of Output in Abaqus/CAE	147
CHAPTER 4	EXPERIMENTAL STUDIES ON 3-D MODELLING OF THE STRUCTURAL OUTRIGGER SYSTEMS	149
4.1	Introduction	149
4.2	Mechanical properties of Material	150
4.3	Experimental 3D Modelling on Structural Outrigger Systems	153
4.4	Performance of the Core Structural Systems Under Quasi-Static Cyclic Test (no Outrigger)	153
4.4.1	Quasi-Static Cyclic Test on the Core-1 Model (no Outrigger, Regular Cross-Section, $H = 2550 \text{ mm}$)	154
	4.4.1.1 The Core-1 Model Failure Mechanism	154
	4.4.1.2 The Core-1 Model Hysteresis Loops and Backbone Curve	156
	4.4.1.3 The Core-1 Model Energy Dissipation and Ductility	158
	4.4.1.4 The Core-1 Model Strain Values from Quasi-Static Cyclic Test	160
4.4.2	Quasi-Static Cyclic Test on the Core-2 Model (no Outrigger, Thicker Cross-Section, $H = 2550 \text{ mm}$)	161
	4.4.2.1 The Core-2 Model Failure Mechanism	162
	4.4.2.2 The Core-2 Model Hysteresis Loops and Backbone Curve	164
	4.4.2.3 The Core-2 Model Energy Dissipation and Ductility	165

4.4.2.4	The Core-2 Model Strain Values from Quasi-Static Cyclic Test	167
4.4.3	Quasi-Static Cyclic Test on the Core-3 (no Outrigger, Regular Cross-Section, $H = 1850 \text{ mm}$)	168
4.4.3.1	The Core-3 Model Failure Mechanism	169
4.4.3.2	The Core-3 Model Hysteresis Loops and Backbone Curve	170
4.4.3.3	The Core-3 Model Energy Dissipation and Ductility	172
4.4.3.4	The Core-3 Model Strain Values from Quasi-Static Cyclic Test	174
4.5	Performance of the Single-Outrigger Systems Under Quasi-Static Cyclic Test	175
4.5.1	Quasi-Static Cyclic Test on Single-Outrigger Optimum Model (Outrigger at $x = 0.5H$)	176
4.5.1.1	One-Outrigger Optimal Form Failure Mechanism	177
4.5.1.2	One-Outrigger Optimal Form Hysteresis Loops and Backbone Curve	180
4.5.1.3	One-Outrigger Optimal Form Energy Dissipation and Ductility	183
4.5.1.4	One-Outrigger Optimal Form Strain Values from Quasi-Static Cyclic Test	185
4.5.2	Quasi-Static Cyclic Test on Single-Outrigger Cap Model (Outrigger at $x = 0$)	187
4.5.2.1	One-Outrigger Cap Model Failure Mechanism	187
4.5.2.2	One-Outrigger Cap Model Hysteresis Loops and Backbone Curve	189
4.5.2.3	One-Outrigger Cap Model Energy Dissipation and Ductility	191
4.5.2.4	One-Outrigger Cap Model Strain Values from Quasi-Static Cyclic Test	193

4.6	Performance of the Two-Outrigger Systems Under Quasi-Static Cyclic Test	195
4.6.1	Quasi-Static Cyclic Test on Two-Outrigger Conventional Model (Outriggers at $x = 0$ & $0.5H$)	196
4.6.1.1	Two-Outrigger Conventional Form Failure Mechanism	197
4.6.1.2	Two-Outrigger Conventional Form Hysteresis Loops and Backbone Curve	198
4.6.1.3	Two-Outrigger Conventional Form Energy Dissipation and Ductility	201
4.6.1.4	Two-Outrigger Conventional Form Strain Values from Quasi-Static Cyclic Test	203
4.6.2	Quasi-Static Cyclic Test on Two-Outrigger Optimal Model (Outriggers at $x = H/3$ & $2H/3$)	205
4.6.2.1	Two-Outrigger Optimal Form Failure Mechanism	206
4.6.2.2	Two-Outrigger Optimal Form Hysteresis Loops and Backbone Curve	207
4.6.2.3	Two-Outrigger Optimal Form Energy Dissipation and Ductility)	213
4.6.2.4	Two-Outrigger Optimal Form Strain Values from Quasi-Static Cyclic Test	215
4.7	Discussion on Experimental Test Results of the Conventional Structural Outrigger Systems	217
4.7.1	Discussion on Experimental Test Results of the Failure Modes of the Conventional Outrigger Models	217
4.7.2	Discussion on Experimental Test Results of the Backbone Curve Capacities of the structural Core Models and Conventional Outrigger Models	219

4.7.2.1	Discussion on Experimental Test Results of the Backbone Carve Capacities of the Core Models	219
4.7.2.2	Discussion on Experimental Test Results of the Core-1, Single Opti-Out, and Multi Opti-Out Models	220
4.7.2.3	Discussion on Experimental Test Results of the Core-2 and Cap-Out Models	221
4.7.2.4	Discussion on Experimental Test Results of the Core-3 and 2-Out Conventional Models	222
4.7.3	Discussion on Experimental Test Results of the Energy Dissipation of the Conventional Outrigger Models	223
4.7.4	Discussion on Experimental Test Results of the Ductility Ratio of the Conventional Outrigger Models	224
4.8	Summary of the First Part of the Experiments	224
CHAPTER 5	EXPERIMENTAL AND NUMERICAL MODELLING IN DEVELOPING A NEW FORM OF STRUCTURAL OUTRIGGER SYSTEM	227
5.1	Introduction	227
5.2	Experimental 3D Modelling of the New Form structural Outrigger System	228
5.3	Performance of the New Form structural Outrigger System Under Quasi-Static Cyclic Test	230
5.3.1	Quasi-Static Cyclic Test on Developed Outrigger Model (Outrigger at $x = 0.5H$)	232
5.3.1.1	Developed Outrigger Model Failure Mechanism	232
5.3.1.2	Developed Outrigger Model Hysteresis Loops and Backbone Curve	234

	5.3.1.3 Developed Outrigger Model Energy Dissipation and Ductility	238
	5.3.1.4 Developed Outrigger Model Strain Values from Quasi-Static Cyclic Test	240
5.4	Numerical 3D Modelling a New Form of the Structural Outrigger Systems Under Quasi-Static Cyclic load	242
	5.4.1 Material Properties	243
	5.4.2 Verification of the Numerical Models (FEM)	244
	5.4.1.1 Validation of Core- 1 Model (Regular Cross-Sectional, H=2550 mm)	245
	5.4.1.2 Validation of Core- 2 Model (Thicker Cross-Sectional, H=2550 mm)	246
5.5	Modelling and Finite Element Analysis (FEA) of the Developed Outrigger Model	248
5.6	FE Analysis on the Simulated Experimental Developed Outrigger Model Under Quasi-Static Cyclic Loading (Outrigger at $x = 0.5H$)	248
	5.6.1 FE Analysis on the Developed Outrigger Model, Failure Mechanism (Under Quasi-Static Cyclic Loading)	249
	5.6.2 FE Analysis on the Developed Outrigger Model, Hysteresis Loops and Backbone Curve	250
	5.6.3 FE Analysis on the Developed Outrigger Model, Energy Dissipation and Ductility	254
5.7	Optimisation of 3D Numerical Simulation of the Proposed New Outrigger Model (Dev-Out Model)	256
	5.7.1 Optimisation of the Deve-Out model (Top-Drift)	257
	5.7.1.1 Numerical Modelling and Optimisation of the Deve-Out model (Top-Drift)	258
	5.7.1.2 Numerical Results on Optimisation of the Dev-Out FE model (Top-Drift)	259
	5.7.2 Optimisation of the Dev-Out Model (Base-Moment)	261

5.8	Numerical Results and Discussion on Optimization	
	Dev-Out Model	262
5.8.1	Comparison on Failure Mechanism on Experimental and FEA models (Dev-Out Model)	263
5.8.2	Comparison on Backbone Curves of the Experimental and FEA models (Dev-Out Model)	263
5.8.3	Comparison on Energy Dissipation and Ductility of the Experimental and FEA models (Dev-Out Model)	264
5.9	Summarized Numeric Results of the Optimization Outrigger Systems	265
5.10	Summary of Experimental and Numerical Findings on Outrigger Structure Systems	266
CHAPTER 6	CONCLUSION	267
6.1	Introduction	267
6.2	Findings of Research	267
6.2.1	Conclusion on the Behaviour of the Conventional Structural Outrigger Systems	268
6.2.2	Development of A New Outrigger Form for Structural Outrigger Systems	269
6.2.3	Optimisation and Evaluation of Developed Outrigger Model Through FEM Modelling	269
6.3	Summarise the Conclusion	269
6.4	Contribute to Knowledge	270
6.5	Recommendations for Future Works	271
	REFERENCES	273

LIST OF TABLES

TABLE NO.	TITLE	PAGE
Table 2.1	The outrigger topology relationship with material, stiffness and strength (Ho, 2016)	25
Table 2.2	The numerically obtained results of the optimum position of outrigger systems in the tall buildings structure by previous researchers	76
Table 3.1	The specifications and dimensions of the prototype models	90
Table 3.2	Comparison of the effects of meshing size for FEA analysis and the experimental result in the top deflections of a core model subjected to the lateral loading	136
Table 4.1	The Engineering results of material properties by the mechanical tensile Test	151
Table 4.2	Stiffness and ductility parameters for the Core-1 model (based on the top displacements)	158
Table 4.3	Ductility for Core-1 based on the top of the experimental model	160
Table 4.4	Stiffness and ductility parameters for the Core-2 model (based on the top displacements)	165
Table 4.5	Ductility for Core-2 based on the top of the experimental model	167
Table 4.6	Stiffness and ductility parameters for the Core-3 model (based on the top displacements, $H = 1850\text{ mm}$)	172
Table 4.7	Ductility for Core-3 based on the top of the experimental model	174
Table 4.8	Stiffness and ductility parameters for the one-outrigger Optimal form (based on the top displacements)	181

Table 4.9	Stiffness and ductility parameters for the one-outrigger optimal form (based on the outrigger level displacements)	182
Table 4.10	Ductility for one-outrigger optimal form based on the top of the experimental model	184
Table 4.11	Ductility for one-outrigger optimal form based on the outrigger level of the experimental model	185
Table 4.12	Stiffness and ductility parameters for the one-outrigger Cap form (based on the top displacements)	191
Table 4.13	Ductility for one-outrigger Cap form based on the top of the experimental model	193
Table 4.14	Stiffness and ductility parameters for the Two-outrigger conventional form (based on the top displacements, Out-1, LM-1 at the top)	199
Table 4.15	Stiffness and ductility parameters for the Two-outrigger conventional form (based on the Out-2 displacements, LM-2 at the mid-height)	201
Table 4.16	Ductility for two-outrigger Conventional form based on the top of the experimental model	203
Table 4.17	Stiffness and ductility parameters for the Two-outrigger optimal form (based on the top displacements, LM-1)	210
Table 4.18	Stiffness and ductility parameters for the Two-outrigger optimal form (based on the Out-1 displacements, LM-2 at the 1/3H from the top)	211
Table 4.19	Stiffness and ductility parameters for the Two-outrigger optimal form (based on the Out-2 displacements, LM-3 at the 2/3H from the top)	213
Table 4.20	Ductility for two-outrigger Optimal form based on the top of the experimental model	215
Table 4.21	Failure locations of the experimental conventional outrigger modes under quasi-static cyclic test	219
Table 4.22	Summary of the results obtained from experimental tests (Objective1)	225

Table 5.1	Stiffness parameters for the developed outrigger model (based on the top displacements)	236
Table 5.2	Stiffness parameters for the developed outrigger model (based on the outrigger level displacements)	238
Table 5.3	Ductility for developed outrigger model based on the top-level of the experimental model	240
Table 5.4	The results of the mechanical material properties by the mechanical tensile test	243
Table 5.5	FE Stiffness parameters for the Dev-Out model (based on the top displacements)	252
Table 5.6	FE Stiffness parameters for the Dev-Out model (based on the outrigger level displacements, H/2)	254
Table 5.7	Ductility for FE Dev-Out model based on the top-level of the simulated model	256
Table 5.8	The results of finite element analysis (FEA) of three-dimensional models.	262
Table 5.9	Comparison of experimental and numerical cumulative energy dissipation capacity of the Dev-Out model	265
Table 5.10	Summary of the findings obtained from experimental and numerical studies	266

LIST OF FIGURES

FIGURE NO.	TITLE	PAGE
Figure 1.1	Schematic of the height increase in high-rise buildings of the world from 1885 to 2010 (Marshall Gerometta, 2009)	2
Figure 1.2	Evolution of structural systems (Buyukozturk and Gunes, 2004)	3
Figure 1.3	Category of dual structural systems (Ali and Moon, 2007)	4
Figure 1.4	The concept of conventional structural outrigger system in the tall building with central core, outrigger and belt truss (Taranath, 2009)	5
Figure 2.1	The use of the outrigger leverage in narrowboats hull fishing to avoid overturning (Choi, et al., 2012a)	14
Figure 2.2	Types of various positions core and outrigger in outrigger structure systems: (a) Cap outrigger structure model, (b) Outrigger structure with offset core, and (c) Outrigger structure with centrally core	15
Figure 2.3	The typical lateral load resisting systems used in reinforced concrete tall buildings (Taranath, 2009)	19
Figure 2.4	The outrigger system, (a) Plan at the outrigger level, (b) Elevation of the outrigger system and (c) Free core alone without the outrigger	23
Figure 2.5	Two types of the delay joints of outrigger connections; (a) steel delay joint and (b) concrete delay joint (Kwangryang Chung, 2015)	26
Figure 2.6	Adjustable steel joints to eliminate shortening column effects (Kwangryang Chung, 2015)	27
Figure 2.7	(a) details of the cross-jack system (Kwok and Vesey, 1997), and (b) cross-jack adjustment after construction (Kwangryang Chung, 2015)	28

Figure 2.8	3D-schematic and 2D-details of the shim plate outriggers connection were used in Cheung Kong Centre (Ho, 2016)	28
Figure 2.9	The retro-method, (a) Embedded truss as a part of the outrigger system in the core walls, (b) Encasing the core walls in the retro-technique and, (c) details the retro-installation of casting the outrigger into the core walls (Wong and Ho)	29
Figure 2.10	Damping outrigger system; (a) Schematic performance concept of the damped outrigger system, (b) detail of damped outrigger level, and (c) installation of the damped outrigger (Smith and Willford, 2008)	30
Figure 2.11	The detail of the fused RC-outrigger systems in tall buildings (Ho, 2016)	31
Figure 2.12	Rotation of the core, axial deformation of the peripheral columns, and bending of the outrigger under lateral load	33
Figure 2.13	Cap outrigger system: (a) Roof plan of building with a central core (b) reverse curvature due to cap outrigger, and (c) lateral deflection of the core alone	34
Figure 2.14	Analytical model of a single outrigger under uniform lateral load	36
Figure 2.15	(a) Outrigger location at the top ($Z = L$), (b) lateral deflection diagrams, (c) the outrigger moment diagram, and (d) final reduced moment diagram	37
Figure 2.16	(a) Outrigger location at ($Z = 0.75L$), (b) lateral deflection diagrams, (c) the outrigger moment diagram, and (d) final reduced moment diagram	39
Figure 2.17	A central cantilever core due to external lateral load W coordinates	39
Figure 2.18	(a) Outrigger location at ($Z = 0.5L$), (b) lateral deflection diagrams, (c) the outrigger moment diagram, and (d) final reduced moment diagram	42

Figure 2.19	(a) Outrigger location at ($Z = 0.25L$), (b) lateral deflection diagrams, (c) the outrigger moment diagram, and (d) final reduced moment diagram	43
Figure 2.20	(a) Two-outrigger structure, (b) bending moment diagram under external load, (c) and (d) restoring moment $M1$ and $M2$, and (e) reduced bending moment diagram due to outriggers	47
Figure 2.21	Approximately optimum location of the outrigger: (a) One-outrigger, (b) Two-outrigger, (c) Three-outrigger, and (d) Four-outrigger (Taranath, 2011).	52
Figure 2.22	The optimum locations graph up to four outriggers systems with respect to ω (Smith and Coull, 1991)	53
Figure 2.23	Performance of the outrigger systems reduces the drift and the base moment with respect to ω (Smith and Coull, 1991).	54
Figure 2.24	Two conventional single outrigger structural forms; (a) cap outrigger at the top, (b) the outrigger at the optimum level	55
Figure 2.25	Two conventional double outriggers structural forms; (a) one outrigger at the top and other at the optimum level, (b) both outriggers at the optimum levels	56
Figure 2.26	Optimum location of an outrigger based on variable relative flexural rigidities (ω vs αH) of the outrigger (Zeidabadi, et al., 2004)	60
Figure 2.27	Optimum location of the outrigger based on parameters of stiffness (Hoenderkamp and Bakker, 2003)	60
Figure 2.28	A similar model that was transformed into the three Finite Element Programs (Wu and Zhang, 2012)	80
Figure 3.1	The flowchart of the proceeding of this research	88
Figure 3.2	Schematic of the outriggers spaces set at intervals of; (a) $H/(N + 1)$ as type (A) no outrigger at the top, (b) (H/N) as type (B) no outrigger at the top and (c) (H/N) as type (C) one outrigger permanent located at the top	90

Figure 3.3	Schematic of the prototype outrigger models	92
Figure 3.4	Laboratory flowchart of the experimental process to conduct the tests	95
Figure 3.5	A schematic form of the general dimensions in three directions of the models, (a) a type of the numerical models, (b) a type of the experimental models	97
Figure 3.6	Dimensions of the new outrigger form with a symmetrical plan, (a) 3D view of the model, (b) details of the experimental sizes of the new model	98
Figure 3.7	To fabricate laboratory specimens, (a) Rectangular tube, (b) Square Tube, (c) Equal Angle, (d) Flat bar Aluminum Profiles, (e) Aluminum Blind Rivets and (f) manual Riveter	100
Figure 3.8	Standard tension test for Aluminium specimens dimensions accordance to ASTM E8 (Standard, 2004b)	102
Figure 3.9	Standard tensile test for three replicated similar aluminum specimens	102
Figure 3.10	Universal testing machine set-up and its details before testing	103
Figure 3.11	Two-rectangular hollow tube sections of the core components, and AL flat bar fastened with rivets spacing	105
Figure 3.12	2D uniform model selective in the approximate analysis method which is subjected to the lateral linear load (Marabi and Marsono, 2016)	106
Figure 3.13	A representative of the proposed scheme of the SRM method on the 3D down-scale modelling of the uniform structures with details	109
Figure 3.14	Prototype experimental 3D models: (a) central core system no outrigger, (b) single-outrigger system, outrigger at mid-height	111

Figure 3.15	Prototype experimental 3D models: (c) cap-outrigger system, (d) two-outrigger system at the optimum location	112
Figure 3.16	Prototype experimental 3D models: (e) two-outrigger system, one outrigger at the top and second at the midheight, and (f) new developed outrigger system	112
Figure 3.17	Schematic set-up for quasi-static cyclic test on the models at Structures Lab.	115
Figure 3.18	Multi-purpose reinforced footing, (a) the steel filler plates to render the fixed support of the central core to the base, (b) welded simple support of the columns, (c) dimensions of the footing, and (d) the completed footing for installing the experimental models	116
Figure 3.19	The multi-purpose RC-Base set-up to test the models	117
Figure 3.20	The set-up of the central core on the RC-base with the steel filler plates as a fixed support	118
Figure 3.21	Set-up and installation of the model with the simple connection of the columns and the fixed support of the core on the RC-Base	119
Figure 3.22	Two hydraulic jack machines as a manual horizontal actuator	120
Figure 3.23	Load cell to record the horizontal forces	121
Figure 3.24	LVDTs at the top and the outrigger locations on the models	122
Figure 3.25	Representative of the inclinometer positions on the models	123
Figure 3.26	TML data logger machine and details of the SG places on the models	124
Figure 3.27	Places of the 4 SGs used at the base and the upper surface of the outrigger connection on the core	126
Figure 3.28	Places of the 6 SGs used at the base, lower, and the upper surface of the outrigger connection on the core of Cap-Out model	127

Figure 3.29	Schematic layout of (a) Laser Meter locations, (b) Inclinator locations, (c) horizontal Hydraulic Jacks and Gravity loads, and (d) Strain Gauge locations for 2-Out Conv Model	128
Figure 3.30	Schematic layout of (a) Laser Meter locations, (b) Inclinator locations, (c) horizontal Hydraulic Jacks and Gravity loads, and (d) Strain Gauge locations for 2-Out Opti Model	129
Figure 3.31	Quasi-static cyclic test and loading directions using two Jacks under the gravity loads simultaneously	132
Figure 3.32	Sell element type; (a) shell element (Manual, 2012) and (b) meshed of shell element specimen	135
Figure 3.33	Cross-Section of proposed outrigger model, (a) double rectangular tube profile sizes of the core element, (b) rectangular tube profile size of the outrigger beam elements and (c) square section profile of the column elements	138
Figure 3.34	(a) Dimensions of the new outrigger model, (b) a schematic Dev-Out model	140
Figure 3.35	Merging the outrigger and central core to create the fixed connection and the MPC pin connection between the outrigger and columns	141
Figure 3.36	The simply supports the outer columns to connect the base and fixed support connection of the central core	142
Figure 3.37	Gravity applied loads (a) the gravity loads at the top of the 3D laboratory model, and (b) imposed concentrated loads at the upper part of the 3D Abaqus simulation	144
Figure 3.38	The FEM developed outrigger proposed modelling by Abaqus/CAE, modelling, boundary conditions and loading	145
Figure 3.39	Scheme of deformation-controlled loading history (FEMA, 2007)	146
Figure 3.40	A general load protocol calculated based on FEMA-461	146

Figure 4.1	Universal testing machine and its details of the fractured sample	150
Figure 4.2	Three fractured material samples due to the tensile test by the universal testing machine	151
Figure 4.3	The stress-strain curves of Engineering and True data from the laboratory test of the used material	152
Figure 4.4	Fully local buckling and losing stiffness in the Core-1 model at the base, buckling at the web and flange (H=2550 mm)	156
Figure 4.5	Hysteresis loops and the backbone curve of the Core-1 Model, based on the top displacement of the model	157
Figure 4.6	Cumulative energy dissipation capacity at different drift values (based on the top displacements of the Core-1 model)	159
Figure 4.7	Lateral force to lateral displacement curve for the Core-1 model test (based on the top-level displacements)	159
Figure 4.8	Strain values of the two SGs used at the base of the Core-1 model	161
Figure 4.9	Failure phenomena at the base of the thicker cross-sectional Core-2 model and buckling at the web and flange (H=2550 mm)	163
Figure 4.10	Hysteresis loops and the backbone curve of the Core-2 Model, based on the top displacement of the model	164
Figure 4.11	Cumulative energy dissipation capacity at different drift values (based on the top displacements of the Core-2 model)	166
Figure 4.12	Lateral force to lateral displacement curve for the Core-2 model test (based on the top-level displacements)	166
Figure 4.13	Strain values of the two SGs used at the base of the Core-2 model	168
Figure 4.14	Failure phenomena of the base of the shorter core with a regular cross-section, buckling at the web and flange (H=1850 mm)	170

Figure 4.15	Hysteresis loops and the backbone curve of the Core-3 Model, based on the top displacement of the model	171
Figure 4.16	Cumulative energy dissipation capacity at different drift values (based on the top displacements of the Core-3 model)	173
Figure 4.17	Lateral force to lateral displacement curve for the Core-3 model test (based on the top-level displacements)	173
Figure 4.18	Strain values of the two SGs used at the base of the Core-3 model	175
Figure 4.19	Fully local buckling and losing stiffness in the central core at the outrigger level before completion of the local buckling at the base of the 1-Out Opti model	179
Figure 4.20	Hysteresis loops and the backbone curve of the 1-Out Opti model, based on the top deflections of the model	181
Figure 4.21	Hysteresis loops and the backbone curve of the single-outrigger optimal form, based on the outrigger level deflections of the model	182
Figure 4.22	Cumulative energy dissipation capacity at different drift values (based on the top displacements of the one-outrigger optimal model)	183
Figure 4.23	Lateral force to lateral displacement curve for the one-outrigger optimal form test (based on the top-level displacements)	184
Figure 4.24	Lateral force to lateral displacement curve for the one-outrigger optimal form test (based on the outrigger level displacements)	185
Figure 4.25	Strain values of the 4 SGs used at the base and outrigger connection on the core in One-Out optimal model in a quasi-static cyclic test	186
Figure 4.26	Local buckling at the base of the central core before at the outrigger place under the quasi-static cyclic test of the one-outrigger Cap form	189
Figure 4.27	Hysteresis loops and the backbone curve of the Cap-Out model, based on the top displacement of the model	190

Figure 4.28	Cumulative energy dissipation capacity at different drift values (based on the top displacements of the one-outrigger Cap model)	192
Figure 4.29	Lateral force to lateral displacement curve for the one-outrigger Cap form test (based on the top-level displacements)	193
Figure 4.30	Strain average values recorded at the base, lower and upper of the outrigger location on the central core of the Cap-Out model through the cyclic test	194
Figure 4.31	Schematic configuration of the Two-Outrigger structural systems concerning the outrigger locations	196
Figure 4.32	Failure mode of the 2-Out Conv Model under quasi-static cyclic test	198
Figure 4.33	Hysteresis loops and the backbone curve of the 2-Out Conv model, based on the top deflections of the model (LM-1)	199
Figure 4.34	Hysteresis loops and the backbone curve of the 2-Out Conv model, based on the second outrigger level deflections (LM-2)	200
Figure 4.35	Cumulative energy dissipation capacity at different drift values (based on the top displacements of the 2-Out Conv model)	202
Figure 4.36	Lateral force to lateral displacement curve for the 2-out Conv model test (based on the top-level displacements, LM-1)	203
Figure 4.37	Strain values of the 8 SGs used at the base and outrigger connection on the core in the 2-Out conv model	205
Figure 4.38	Failure mode of the 2-Out Opti Model under quasi-static cyclic test	207
Figure 4.39	Hysteresis loops and the backbone curve of the Two-Outrigger Optimal form, based on the top deflections of the model (LM-1)	209

Figure 4.40	Hysteresis loops and the backbone curve of the 2-Out Opti model, based on the Out-1 deflections of the model (LM-2)	211
Figure 4.41	Hysteresis loops and the backbone curve of the 2-Outtrigger Opti model, based on the Out-2 deflections of the model (LM-3)	212
Figure 4.42	Cumulative energy dissipation capacity at different drift values (based on the top displacements of the 2-out Opti model)	214
Figure 4.43	Lateral force to lateral displacement curve for the Two-outtrigger Optimal form test (based on the top-level displacements, LM-1)	214
Figure 4.44	Strain values of the 10 SGs used at the base and outrigger connection on the core in the 2-Out Opti model	216
Figure 4.45	Comparison of the force vs displacement curves for the structural Core-1, Core-2 and Core-3 models (based on the top level)	220
Figure 4.46	Comparison of the force vs displacement curves for the Core-1, 1-Out Opti, and 2-Out Opti models	221
Figure 4.47	Comparison of the force vs displacement curves for the Core-2 and Cap-Out models	222
Figure 4.48	Comparison of the force vs displacement curves for the Core-3 and 2-Out Conv models	223
Figure 5.1	Schematic and dimensions of the new outrigger model with a symmetrical plan	229
Figure 5.2	Experimental modelling details of the developed outrigger model (the proposed new form of the structural outrigger systems)	231
Figure 5.3	Fully local buckling and losing stiffness in the central core at the upper outrigger level of the Dev-Out model	234

Figure 5.4	Hysteresis loops and the backbone curve of the developed outrigger model, based on the lateral displacement at the top of the model	235
Figure 5.5	Hysteresis loops and the backbone curve of the developed outrigger model, based on the outrigger level deflections of the model	237
Figure 5.6	Cumulative energy dissipation capacity at different drift values (based on the top displacements of the developed outrigger model)	239
Figure 5.7	Lateral force to lateral displacement curve for the developed outrigger model test (based on the top-level displacements)	240
Figure 5.8	Strain values of the SGs used at the base and outrigger connection on the core in the developed outrigger model in a quasi-static cyclic test	242
Figure 5.9	Non-linear true stress-strain curve of the material (Al) by mechanical tensile test	244
Figure 5.10	Validation of experimental and FEA models of the Core-1 model	246
Figure 5.11	Validation of experimental and FEA models of thicker cross-sectional core- 2 Model	247
Figure 5.12	The plot contours on the deformed shape of the Dev-Out FE model under quasi-static cyclic loading	250
Figure 5.13	Hysteresis loops and the backbone curve of the Dev-Out FE model, based on the lateral displacement at the top of the model	252
Figure 5.14	Hysteresis loops and the backbone curve of the Dev-Out FE model, based on the outrigger level displacements	253
Figure 5.15	FE Dev-Out model cumulative energy dissipation capacity at different drift values (based on the top displacements of the model)	255

Figure 5.16	Lateral force to lateral displacement curve for the Dev-Out FE model (based on the top-level displacements)	256
Figure 5.17	The developed outriggers positions in the 3D Dev-Out FE model	259
Figure 5.18	Numerical capacity curves; Top deflections vs Lateral force of the 3D Dev-Out FE model with different positions from the top of the model	260
Figure 5.19	Optimization curve; top-displacement vs outrigger location at the Dev-Out FE models	261
Figure 5.20	Base moment vs outrigger positions of the Dev-Out model	262
Figure 5.21	Force vs displacement curves for experimental and numerical of the Dev-Out model under quasi-static cyclic loading	264

LIST OF ABBREVIATIONS

2D	Two- Dimensional
3D	Three-Dimensional
BIM	Building Information Modeling
FE	Finite Element
FEA	Finite Element Analysis
FEM	Finite Element Modelling
LDP	Linear Dynamic Procedure
LSP	Linear Static Procedure
NLFEA	Nonlinear Finite Element Analysis
RC	Reinforced Concrete

LIST OF SYMBOLS

A	Width of equivalent strut
A_{inf}	Cross sectional area of infill wall
$A_{opening}$	Area of opening in infill wall
A_{panel}	Area of infill wall
D_u	Ultimate deflection
D_y	Yield deflection
E	Elasticity modulus of concrete
E_{frm}	Elasticity modulus of frame
E_{inf}	Elasticity modulus of infill
E_m	Modulus of elasticity of masonry
E_0	Modulus of elasticity in linear part of stress strain curve
f'_c	Compression strength for concrete
f'_l	Other field variables
f'_m	Masonry compressive strength
f'_s	Lateral forces
f'_v	Shear stress of full infill wall
G	Modulus of rigidity
h_{eff}	Height of the story
h_{inf}	Height of the infill wall
h_{col}	Height of column
h_{beam}	Depth of beam
$k_{concrete}$	Stiffness of concrete
k_{inf}	Stiffness of infill wall
k_i	Initial stiffness
k	Reduce stiffness
k_{eff}	Effective stiffness
k_p	Post-yield stiffness
L	Length
L_{inf}	Diagonal length of infill
M	Mass

r_{inf}	Shear stress on net area
T	Time
t_{inf}	Thickness of the infill wall
S	Spacing of section bar in column
S_1	Stress at 50×10^{-6} longitudinal strain
S_2	0.4 Compressive strength of concrete
β	Ratio of strength of frame to strength of infill
τ	Shear stress on net area
ε_1	Longitudinal strain at S_1
ε_2	Longitudinal strain at S_2
ε_{t1}	Lateral strain at $0.4 f'_c$
ε_{t2}	Lateral strain at S_1
ρ_w	Width reduction factor of strut
γ	Shear strain
θ	Angle of diagonal of infill with horizon
μ	Ductility
ν	Poisson's ratio of concrete

LIST OF APPENDICES

APPENDIX NO.	TITLE	PAGE
Appendix A	Foundation Procedure	283
Appendix B	Material Properties	287
Appendix C	Loading Protocol	293

CHAPTER 1

INTRODUCTION

1.1 Background of the Study

The construction of tall buildings and towers has become symbolic and application aspects. Since ancient times to the present, high-rise buildings have been of human interest, and in less than half a recent century, it develops faster than the building codes themselves. This change was primarily due to the response to commercial needs close to cities' centers. Another tall building indicator needs include management for business, tourist attractions, and hotels with a detailed, favorable economic return. On the other hand, the rapid growth in the urban population and the rising cost of land and less agricultural activities make the city's horizontal expansion unbearable. The advent of high-quality materials such as composite, steel, and concrete has resulted in a lightweight and slender frame construction that longs to increase buildings' height, as shown in Figure 1.1.

After World War II, particular interest to increase the height of buildings has triggered an introduction of various new high-performance structural systems using high-strength materials. Gradually, unique structural systems and curved structural members such as columns, beams, and shear walls have to lead to freedom in the architecture and design of systems. The role of the advanced structural analysis software and Building Information Modeling (BIM) has assisted this progress. However, in the structural engineering perspective, high-performance structures and appropriate construction methods regarding bearing systems have created the adverse effects of increasing the structures' height.

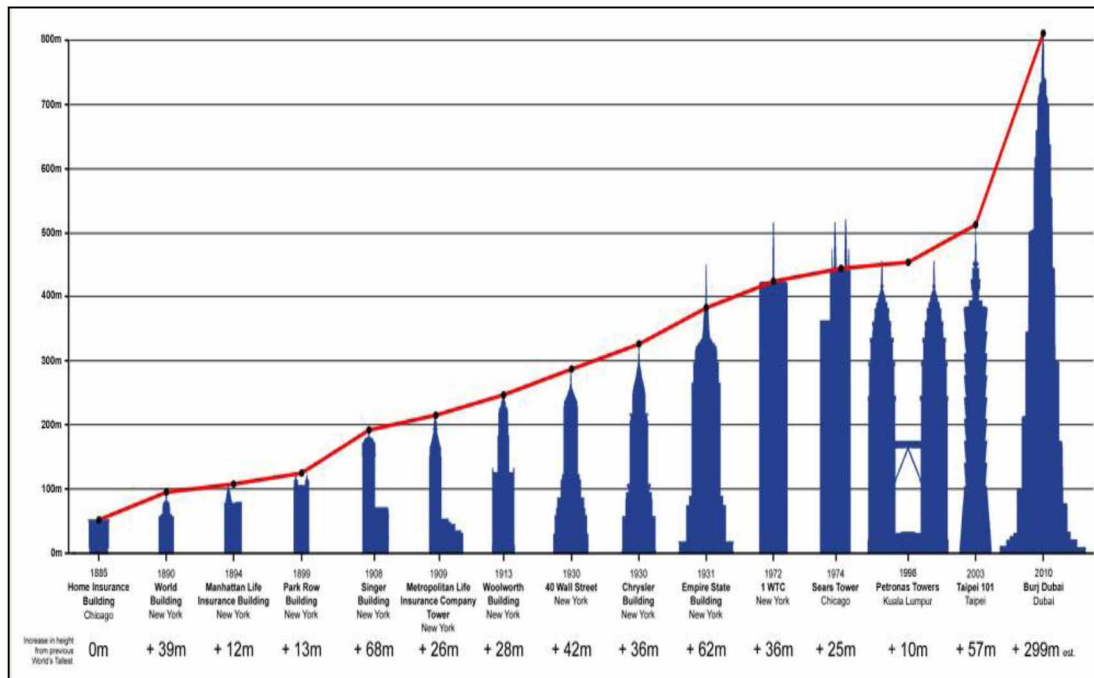


Figure 1.1 Schematic of the height increase in high-rise buildings of the world from 1885 to 2010 (Marshall Gerometta, 2009)

The primary role of tall buildings structures is to carry the gravity loads and the lateral loads, statically or dynamically. Duo to the destructive effects of lateral loads (earthquake or wind) over a building's life, it is necessary to provide a robust structural system that should also be economical and stable. The secondary effect led to the overturning of the structures by the lateral load's act. This force is directly related to the ratio of the squares of the height increases of the structure. In this regard, the development and evolution of tall structural systems with the resisting shear core walls as a lateral load's resisting system was combined with other structures since 1960' S, as shown in Figure 1.2.

The concept of a tall building is known as a cantilever structure. They are designed to carry loads, stiffness, strength, and ductility (Al-Subaihawi, Kolay et al. 2020). However, top-drift control is essential for designing tall building structures (Günel and Ilgin 2014). Dual structures such as structural outrigger systems are usually combined with other structural forms to enhance performance against the lateral loads.

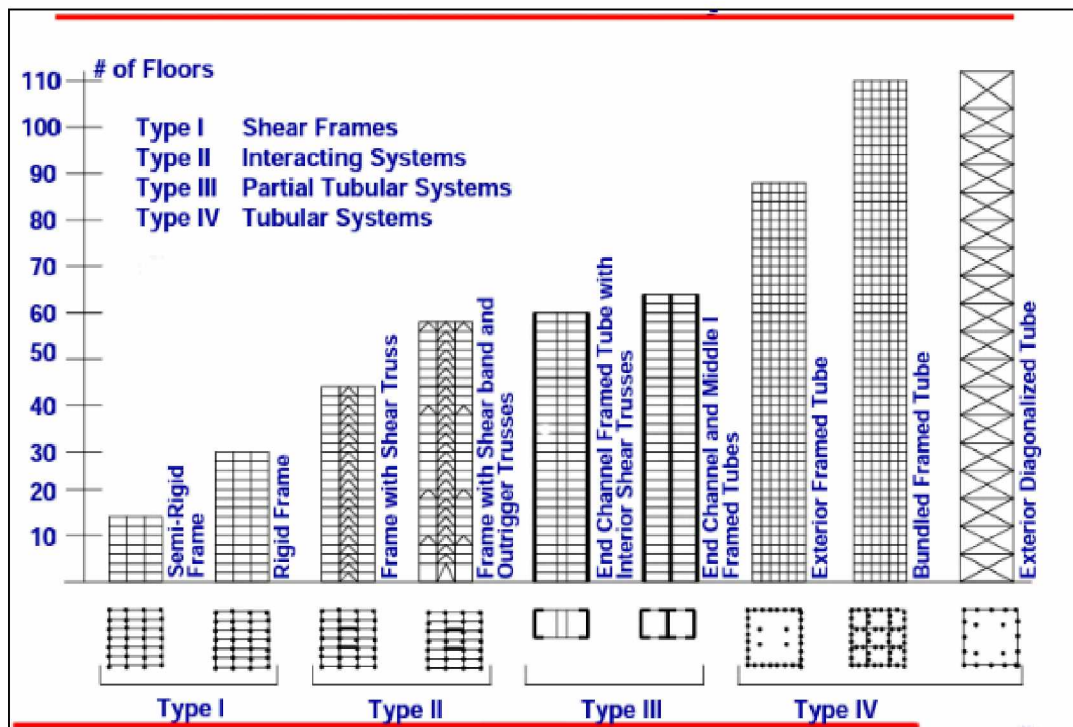


Figure 1.2 Evolution of structural systems (Buyukozturk and Gunes, 2004)

The gradual growth up of the development and evolution of dual tall structural forms are shown in Figure 1.3.

One of the functions that the lateral load resisting system could enhance in tall buildings is using a structural outrigger system. Utilizing an outrigger beams connection to the core-frame systems to create a strength couple to the external columns. The outrigger systems increase the flexural stiffness's effective depth in the lateral load resisting system of the tall building's structure as a vertical cantilever structure (Taranath 2011). The outriggered structural systems resist rotation and overturning moments of the building compared to a conventional structural system (Chen and Zhang 2018). The performance of the tall buildings structures associated with the outrigger systems could obviate this problem.

Among the tall buildings globally, most high-rise buildings with heights ranging from 40-to-100 floors are usually mixed-use (Fatima, Fawzia et al. 2011, Moon 2011). In high-rise buildings with such height, the outrigger systems are frequently applied, effectively decreasing the top drift from a lateral load such as wind or earthquake loads (Mazzotta, Brunesi et al. 2017). The use of the outrigger systems

is necessary, especially in tall buildings above 100 stories. Creating an outrigger system combined with peripheral columns is often adopted to resist high-rise buildings' lateral load resisting system (Mohamed and Najm 2016).

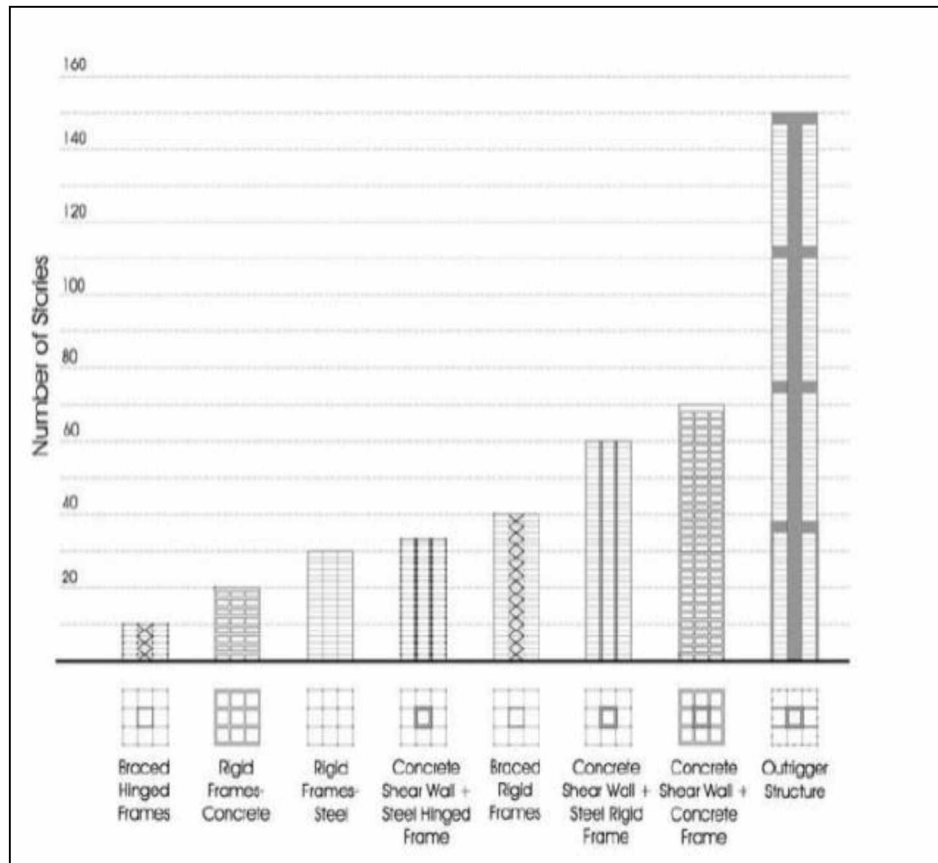


Figure 1.3 Category of dual structural systems (Ali and Moon, 2007)

This study investigates the slender structure in high-rise buildings by using the outrigger systems to create the lateral load resisting systems and minimize horizontal roof displacement. Application of the outrigger systems could also enhance the buildings' lateral stiffness without changing their component sizes or increasing their mass. The slender buildings or narrow-tall building usually forms inner shear core walls as a primary lateral resisting system. The outrigger element is coupled to the core with the external columns making it a big rigid body. Thus, components of the structural outrigger systems can include a central core, outrigger beams, and peripheral columns. An outrigger element can be a deep beam, concrete wall, or truss that occupied one or two-story height. It is duplicated at one or a few levels throughout the structure's total height, as shown in Figure 1.4.

With this new concept in design and construction, many countries constructed enormous capital cities' structures. For example; Taipei in Taiwan in 2010 with a 510m height, Petronas Twin Towers in Malaysia in 1998 with a 452 m height, The Shanghai Tower in 2015 with a 632 m height and 124 levels with six outrigger levels, the skyscraper of Burj Dubai in 2010 with an 828m height, and Jeddah Tower in 2018 with a height that exceed 1000 m were completed (Lee, Shin et al. 2018).

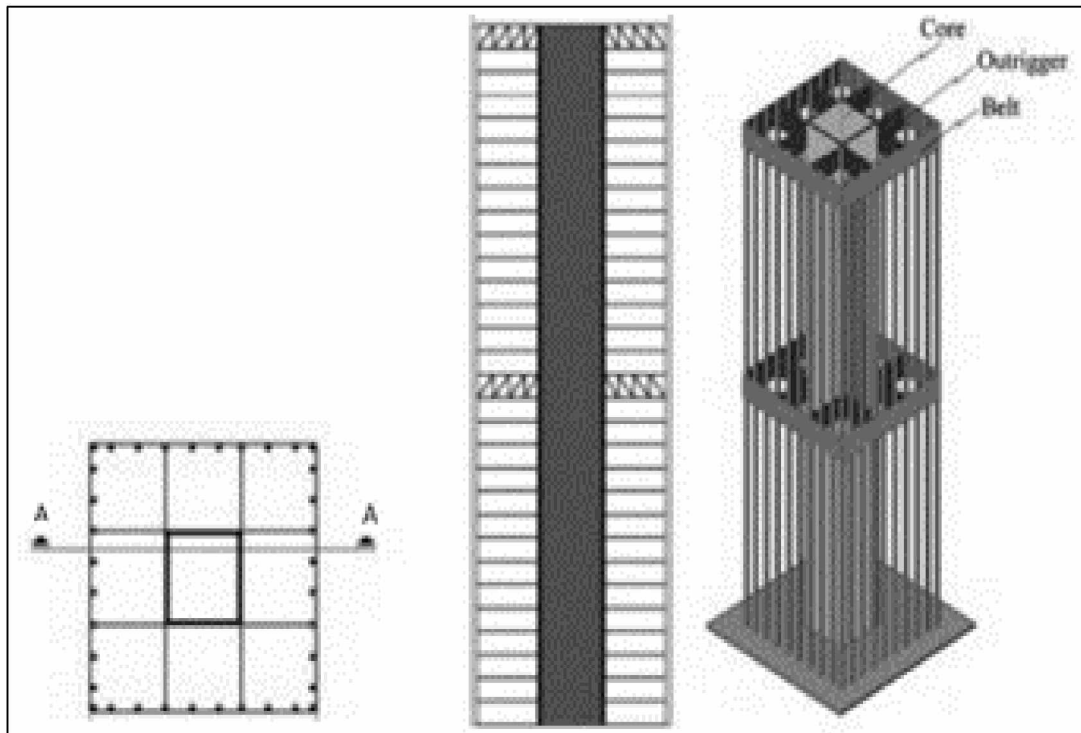


Figure 1.4 The concept of conventional structural outrigger system in the tall building with central core, outrigger and belt truss (Taranath, 2009)

The structural outrigger systems' experimental-theoric performance as a dual-structural system under quasi-static cyclic loads in the tall buildings was examined in this research. They considered that the tall buildings' primary lateral load resistance systems had been a resisting central core. In this way, an outrigger system combined with a structural core system has considered creating a dual system as a lateral load resisting structural outrigger system. In combination with the central core, the mechanism of the outrigger system is using deep beam concepts. The deep beams were fixed to the central core and pinned to the peripheral columns. Conventional outrigger models versus the developed outrigger model investigated the capacity and performance of the outrigger systems. This study examines a new type of outrigger

system's ability to mitigate lateral deflection in a tall building structure compared to conventional outrigger models. The developed model has added an extra column after the core and perimeter columns to extend the width and enhance its stiffness on both sides of the building. The effectiveness of a new type of outrigger system efficiency was compared to conventional models through experimental works.

1.2 Statement of the Problem

Vertical growth of the modern cities for land scarcity and the limit of urban habitats' horizontal progress become significant. Construction of the high-rise building is progressing as competition in the globe. The lateral deflections mitigation of the tall buildings or mainly top-displacement control of the buildings is a significant challenge in choosing the type and design of high-rising construction structures. Utilizing the different types of structures with high-quality, new materials and lightweight could not solve the problem unless using an enhanced structural technique. Using the structural outrigger systems to support the lateral load resisting frames often as a particular structural system has been the best choice for this problem. Determining the best-fit place of the outrigger locations to obtain high efficiency in reducing the building's top-drift due to horizontal forces is another problem. Preventing the destructive effects of lateral loads is another problem as well. For this purpose, using the structural outrigger systems could raise the building's height without increasing the mass and changing the size of the structure's components to satisfy the problem.

In this research, the lateral load resisting system in tall buildings structure utilizing the outrigger systems has been investigated. An innovative method to increase accuracy was followed by converting the 2D basic theoretical models to three-dimensional (3D) modelling. Experimental works and 3D numerical modelling on the conventional outriggered frames are considered to respond to all conventional 2D models' theoretical methods. In this study, the structural outrigger systems' theoretical conventional method is examined to develop experimental 3D models to compare the accuracy of this method. The accuracy of the 3D modeling method is able to response of the stiffness demand for designers in the tall buildings compared to the 2D

modelling to eliminate problem-solving assumptions in the previous traditional methods that are applicable to optimize the structural outrigger systems.

The conventional outrigger systems can not completely solve the problem of lateral stiffness of high-rise buildings. A developed type of the outrigger structures had been proposed in which is a column row added after the peripheral columns with extending outrigger length that led to increase the wide of the building. The proposed new outrigger structure model increased the structure's depth of flexural rigidity and to increase the lateral load resisting system in tall buildings. In this research, a new system is proposed to able to improve the lateral stiffness and top-drift problem. The conventional outrigger systems compared to the proposed outrigger system are evaluated. In both models, the efficiency of the outriggers to minimize the top-drift was investigated. The lateral capacity of the structural outrigger systems to respond to the seismic loads needs to propose a highly efficient new model. The obvious is that previous studies show that the researchers have ignored this matter.

Due to the complexity of traditional equations analysis of the interaction between the core action, outriggers, and columns in the outriggered frame, an advanced Finite Element (FE) software program is required. The numerical analysis procedures are appropriate alternatives at the actual conceptual in the structural design comparable to estimated costs and save times versus the traditional methods and experimental works. This way, investigating numerical parameters affecting the proposed new outrigger model's efficiency under quasi-static cyclic load is needed. The 3D simulation proposed experiment model of the proposed the new outrigger model must be compared and validated to save the cost and time.

1.3 Objectives of the Study

This study's main objectives are experimenting with conventional models and developing a new type of outrigger systems in tall buildings structures to increase the lateral load resisting system. In this research, utility a new technique on the scale-down simplified 3D models (SRM) using the experimental works and numerical analysis

(FEA). The performance of structural outrigger systems under the quasi-static cyclic test and an investigation of the factors affecting the lateral stiffness and efficiency in reducing drift at the top of the buildings. The objectives of this research are as follows:

- i. To compare the lateral response of the optimum and conventional outrigger models through experimental works
- ii. To develop a new type of outrigger system and compare its stiffness and location effectiveness with the conventional models through experimental works
- iii. To conduct a sensitivity analysis of the stiffness and outrigger place parameters affecting the lateral response of the developed outrigger system through FEM

1.4 Scope of the Study

The scope comprises the experimentally and numerically response of the conventional models of the outriggered structural systems in tall buildings under quasi-static cyclic loads. A proposed new type of outrigger model is investigated to examine its effective parameters compared to conventional forms. This research focuses on the experimental analysis of 9 scale-down models of the structural outrigger systems with different forms. The primary experiment models were performed as follows:

- A core structural system, Core-1 model (no Outrigger, Regular Cross-Section, H = 2550 mm) with a duplicate model
- A core structural system, Core-2 model (no Outrigger, Thicker Cross-Section, H = 2550 mm)
- A core structural system, Core-3 model (no Outrigger, Regular Cross-Section, H = 1850 mm)

- One-Outrigger system, Conventional Model (Outrigger at $x = 0.5H$, $H = 2550$ mm, $B = 850$ mm)
- One-Outrigger system, Cap-Outrigger Model (Outrigger at $x = 0H$, $H = 2550$ mm, $B = 850$ mm)
- Two-Outrigger system, Optimal Model (Outriggers at $x_1 = H/3$, $x_2 = 2H/3$, $H = 2550$ mm, $B = 850$ mm)
- Two-Outrigger system, Conventional Model (Outriggers at $x_1 = 0H$, $x_2 = H/2$, $H = 1850$ mm, $B = 850$ mm)
- One-Outrigger developed system, New Model (Outrigger at $x_1 = H/2$, $H = 2550$ mm, $B = 1275$ mm), a row-column added after the peripheral columns with extended the outrigger length

The accuracy and efficiency performance of the 3D conventional models and the proposed new model will be verified by conducting quasi-static cyclic loading on the approximately 1:100 scale models in the laboratory. The down-scaled models' geometric dimensions are considered by the aspect ratio ($H/B=3$), where H is the height, and B is the building's width. The experimental models' fabrication is used by available ordinary Aluminum (Al) profiles in the Malaysian market (Alloy 6061 T6). The effect of gravitational loads is considered as a self-weight structure. The models' experimental behavior with imposed fixed vertical load under the lateral loads is evaluated to fully achieve the relationship of force versus displacement responses and failure mode mechanism. A general foundation was provided for the models that were restrained against the movement. A point load is applied horizontally at the top of the models through incremental reversing loading and unloading until the models' full failure.

The numerical simulations were analyzed by the Abaqus (CAE) program. Nonlinear Finite Element Analysis (NLFEA) through ABAQUS software version

6.11-1 is conducted on the models. To achieve the study's objectives and save time is required, three-dimensional Finite Element Analysis (FEA) models of outrigger systems simulate similarly to the experimental models. The quasi-static cyclic loading is undertaken with loading protocol compliance with FEMA 440 Code. The experimental models under reverse quasi-static cyclic tested similar to the numerical analysis.

1.5 Significance of the Study

This research is evident and essential to enhance structural outrigger systems' rigidity and increasing performance in tall buildings structures to decrease lateral deflections due to horizontal forces. Although there are currently high-strength and lightweight materials for construction, it may not be sufficient to increase lateral stiff in structural systems in tall buildings unless using the outrigger technique. The significant issues that would be gained:

1. Present a developed new type of outrigger model for tall- structures with a row-column added after the peripheral columns with extended the outrigger length.
2. It can be achieved by constructing a larger size of tall buildings instead of slender buildings and consequently to design structures due to a decrease in mass towards raising the height.
3. Suggest a new configuration of the outrigger system in tall buildings associated with shear wall core compared to the outrigger systems' conventional shape.

1.6 Thesis Layout

A summary description of this thesis is divided into six main chapters that consist of the written research report: Chapter 1 is a concise introduction of the

structural outrigger systems followed by a statement of the study's objectives and scope. Chapter 2 is presented in a review of structural outrigger systems and relevant research works of reinforced concrete shear core walls with an outriggered structure in tall buildings. Chapter 3 is the experimental and numerical studies' methodology and includes the models' outrigger systems details, materials properties, load protocols, test conducting, discussion on other equipment testing issues. The numerical analysis method and simulate procedure Abaqus/CAE program are presented in details.

Chapter 4 were presented in the experimental work results are presented and discussed. The experimental results in the format of the ultimate capacity of outrigger braced, outrigger connections, the behavior of models, failure mode, cumulative energy dissipation, ultimate lateral load capacity, lateral displacement of the outrigger models are presented. The results were compared with the experiments to validate the accuracy of the proposed 3D modelling and discussions. Chapter 5 focuses on the experimental proposed new outrigger model, and FEA results employ Abaqus software. The 3D modelling outputs in terms of lateral capacity, failure modes, the strain of outrigger connections, the perimeter columns' axial capacity, load-displacement curves, hysteresis loops and backbone curve are discussed and compared with experimental results. Chapter 6 are presented the principal conclusions regarding the effects of using outriggers with resistant central core structures in tall buildings in the earthquake areas and recommendations drawn from this research.

REFERENCES

- Abdul Karim Mulla, S. B. (2015). A Study on Outrigger System in a Tall RC Structure with Steel Bracing. Proceedings of the 2015 International Journal of Engineering Research and Technology: ESRSA Publications,
- ABAQUS, C. (2012). Analysis user's manual, Version 6.12. ABAQUS. Inc.
- Agency, F. E. M. (2007). Interim Testing Protocols for Determining the Seismic Performance Characteristics of Structural and Nonstructural Components. Federal Emergency Management Agency Washington, DC.
- Ajinkya Prashant Gadkari, N. G. G. (2016). Review on Behaviour of Outrigger Structural System in High-Rise Building. International Journal of Engineering Development and Research. 4(2), 9.
- AL, R. A. and HASAN, J. (2016). Behavior of beam and wall outrigger in high -rise building and their comparison. International Journal of Civil, Structural, Environmental and Infrastructure Engineering Research and Development (IJCSEIERD). 6(1), 19-30.
- Ali, M. M. and Moon, K. S. (2007). Structural developments in tall buildings: current trends and future prospects. Architectural Science Review. 50(3), 205-223.
- Al-Subaihawi, S., C. Kolay, T. Marullo, J. M. Ricles and S. E. Quiel (2020). "Assessment of wind-induced vibration mitigation in a tall building with damped outriggers using real-time hybrid simulations." Engineering Structures 205: 110044.
- Andersson, A. and Malm, R. (2004). Measurement evaluation and FEM simulation of bridge dynamics.
- Bayati, Z., Mahdikhani, M. and Rahaei, A. (2008b). Optimized Use of Multi Outriggers System to Stiffen Tall Buildings. Proceedings of the 2008b The 14th World Conference on Earthquake Engineering, October, 12-17.
- Bennett, D. and Steinkamp, J. R. (1995). Skyscrapers: form & function. Simon & Schuster.

- Bentz, A. and Kijewski-Correa, T. (2012). Finite element modeling of tall buildings: The importance of considering foundation systems for lateral stiffness. Proceedings of the 2012 Proc. The 2012 Structures Congress, 20th Analysis and Computation Specialty Conference, Chicago, IL, USA, 207-218.
- Berkeley, C. (2012). CSI analysis reference manual, version 15.
- Bisch, P., Carvalho, E., Degee, H., Fajfar, P., Fardis, M., Franchin, P., Kreslin, M., Pecker, A., Pinto, P. and Plumier, A. (2012). Eurocode 8: seismic design of buildings worked examples. Joint Research Centre European Union, Luxembourg Google Scholar.
- Bishal Sapkota, S. R. S. a. J. T. M. (2017). Comparative Study on Seismic Performance of High-Rise Building With Energy Dissipation and Outrigger Belt Truss System. IJCIET. 8(4), 7.
- Brownjohn, J. M., Xia, P.-Q., Hao, H. and Xia, Y. (2001). Civil structure condition assessment by FE model updating: methodology and case studies. Finite elements in analysis and design. 37(10), 761-775.
- Bungale, S. T. and Taranth, B. (1988). Structural analysis and design of tall building. New York: The William Byrd Press.
- Buyukozturk, O. and Gunes, O. (2004). High-Rise Buildings: Evolution and Innovations. Proceedings of the 2004 Keynote Lecture, CIB2004 World Building Congress, Toronto, Canada,
- Byrne, B. M. (2001). Structural equation modeling: Perspectives on the present and the future. International Journal of Testing. 1(3-4), 327-334.
- Chambers, J. and Kelly, T. (2004). Nonlinear dynamic analysis—the only option for irregular structures. Proceedings of the 2004 13th World Conference on Earthquake Engineering,
- Chen, Y. and Z. Zhang (2018). "Analysis of outrigger numbers and locations in outrigger braced structures using a multiobjective genetic algorithm." The Structural Design of Tall and Special Buildings 27(1): e1408.
- Choi, H. S. and Joseph, L. (2012). Outrigger system design considerations. International Journal of High-Rise Buildings. 1(3), 237-246.
- Choi, H. S., Ho, G., Joseph, L. and Mathias, N. (2012a). Outrigger design for high-rise buildings. Chicago: Council of tall buildings and urban habitat.
- Choi, H. S., Ho, G., Joseph, L. and Mathias, N. (2012b). Outrigger Design for High-rise Buildings. CTBUH.

- Chopra, A. K. and Goel, R. K. (2002). A modal pushover analysis procedure for estimating seismic demands for buildings. *Earthquake Engineering & Structural Dynamics*. 31(3), 561-582.
- Chung, Y. K. (2010). Optimization of Outrigger Locations in Tall Buildings Subjected to Wind Loads. MSc, University of Melbourne, Australia.
- Comartin, C. D., Niewiarowski, R. W. and Rojahn, C. (1996). Seismic evaluation and retrofit of concrete buildings. (Vol. 1) Seismic Safety Commission, State of California.
- Comartin, C. D., Niewiarowski, R. W. and Rojahn, C. (1996). Seismic evaluation and retrofit of concrete buildings. (Vol. 1) Seismic Safety Commission, State of California.
- Coull, A. and W. O. Lau (1989). "Analysis of Multioutrigger-Braced Structures." *Journal of Structural Engineering* 115(7): 1811-1815.
- Council, A. T., M.-A. E. Center, M. C. f. E. E. Research, P. E. E. R. Center and N. E. H. R. Program (2007). Interim Testing Protocols for Determining the Seismic Performance Characteristics of Structural and Nonstructural Components, Federal Emergency Management Agency.
- de Normalisation, C. E. (2000). Concrete. Part 1: Specification, performance, production and conformity. EN206-1, CEN. 69.
- Designation, A. "E8/E8M-09, Standard test methods for tension testing of metallic materials." American association state highway and transportation officials standard AASHTO(T68): 1-3.
- EN, B. (2001). 10002-1: 2001. Tensile Testing of Metallic Materials. Method of Test at Ambient Temperature.
- EN1998-1 (2005). Eurocode 8: Design of structures for earthquake resistance-part 1: general rules, seismic actions and rules for buildings.
- Esposito, R., K. Terwel, G. Ravenshorst, H. Schipper, F. Messali and J. Rots (2017). Cyclic pushover test on an unreinforced masonry structure resembling a typical Dutch terraced house. 16th World Conference on Earthquake, WCEE.
- Fatima, T., Fawzia, S. and Nasir, A. (2011). Study of the effectiveness of outrigger system for high-rise composite buildings for cyclonic region. Proceedings of the 2011 ICECECE 2011: International Conference on Electrical, Computer, Electronics and Communication Engineering: WASET, 937-945.

- Fawzia, S. and Fatima, T. (2010). Deflection control in composite building by using belt truss and outriggers system. Proceedings of the 2010 Proceedings of the 2010 World Academy of Science, Engineering and Technology conference,
- FEMA, A. (2007). 461/Interim Testing Protocols for Determining the Seismic Performance Characteristics of Structural and Nonstructural Components. Applied Technology Council, Redwood City, CA. 113.
- FEMA, F. (1997). 273: NEHRP Guidelines for the seismic rehabilitation of buildings. Federal Emergency Management Agency.
- FEMA., E. U. F. E. M. A. (2000). Prestandard and commentary for the seismic rehabilitation of buildings. FEMA.
- FEMA., O. (1997). NEHRP Commentary on the Guidelines for the Seismic Rehabilitation of Building. FEMA.
- FEMA-356 (2000). volume 1. redwood city, California: applied technology council (report no 40).
- Gerasimidis, S., Efthymiou, E. and Baniotopoulos, C. (2009). Optimum outrigger locations of high-rise steel buildings for wind loading. FLORENCE ITALY JULY 19t h-23r d. 21.
- Ghosh, S. K., Fanella, D. A. and Rabbat, B. G. (1996). Notes on ACI 318-95, Building Code Requirements for Structural Concrete: With Design Applications. Portland cement association.
- Günel, M. H. and H. E. Ilgin (2014). Tall Buildings: Structural Systems and Aerodynamic Form, Routledge.
- Günel, M. H. and Ilgin, H. E. (2014). Tall Buildings: Structural Systems and Aerodynamic Form. Routledge.
- Haghollahi, A., Ferdous, M. B. and Kasiri, M. (2012). Optimization of outrigger locations in steel tall buildings subjected to earthquake loads. Proceedings of the 2012 The 15th World Conference on Earthquake Engineering, Lisboa,
- Harbert, L. (2002). Home Insurance Building-The First Skyscraper. Journal of American Society of Civil Engineers (ASCE). 43(2), 1-2.
- Herath, N., Haritos, N., Ngo, T. and Mendis, P. (2009). Behaviour of outrigger beams in high rise buildings under earthquake loads. Proceedings of the 2009 Australian Earthquake Engineering Society 2009 Conference,

- Hibbitt, H., Karlsson, B. and Sorensen, P. (2012). Abaqus v6. 12 documentation—ABAQUS analysis user's manual. Providence (RI): Dassault Systèmes Simulia.
- Ho, G. W. (2016). The evolution of outrigger system in tall buildings. *International Journal of High-Rise Buildings*. 5(1), 21-30.
- Hoenderkamp, J. (2008). Second outrigger at optimum location on high-rise shear wall. *The structural design of tall and special buildings*. 17(3), 619-634.
- Hoenderkamp, J. and Bakker, M. (2003). Analysis of high-rise braced frames with outriggers. *The structural design of tall and special buildings*. 12(4), 335-350.
- Initiative, T. B. (2010). Guidelines for performance-based seismic design of tall buildings. Pacific Earthquake Engineering Research Center.
- Irfan Moinuddin, A. K. (2013). A Study For The Optimum Location Of Outriggers For High-Rise Concrete Buildings. *International Journal of Advanced Trends in Computer Science and Engineering*. 2(Special Issue of ICACSE 2013), 628 - 633.
- Jahanshahi, M. and Rahgozar, R. (2013). Optimum location of Outrigger-belt Truss in Tall Buildings Based on Maximization of the Belt Truss Strain Energy. *International Journal of Engineering*. 26(7), 693-700.
- Jahanshahi, M., Rahgozar, R. and Malekinejad, M. (2012). A simple approach to static analysis of tall buildings with a combined tube-in-tube and outrigger-belt truss system subjected to lateral loading. *International Journal of Engineering*. 25(3), 289-299.
- Jayaramappa, N. and Karthik.N.M (2014). optimum position of outrigger system for high raised rc buildings using etabs 2013.1. 5 (push over analysis).
- Kafina, R. and J. Sagasetta (2019). “Analysis of outrigger-braced reinforced concrete supertall buildings: Core-supported and tube-in-tube lateral systems.” *The Structural Design of Tall and Special Buildings* 28(1): e1567.
- Kamath, K., Avinash, A. and Upadhyaya, S. (2014). A Study on the performance of multi-outrigger structure subjected to seismic loads. *IOSR Journal of Mechanical and Civil Engineering (IOSR-JMCE)*. 27-32.
- Kamath, K., Divya, N. and Rao, A. U. (2012). A study on static and dynamic behavior of outrigger structural system for tall buildings. *Bonfring international journal of industrial Engineering and Management Science*. 2(4), 15.

- Kamruzzaman, M. and Sazzad, M. M. (2002). Drift minimization of tall building frames. Proceedings of the 2002 27th conference on our world in concrete & structures, 29-30.
- Kei, D. K., Marsono, A. K. and Anang, R. Cyclic Pushover Behaviour on Industrialised Building System Lightweight Blockwork.
- Khanorkar, A. A., Denge, M. S. and Raut, S. (2016b). Belt Truss as Lateral Load Resisting Structural System for Tall Building: A Review.
- Khanorkar, A., Sukhdeve, S., Denge, S. and Raut, S. (2016a). Outrigger and Belt Truss System for Tall Building to Control Deflection: A Review. GRD Journals-Global Research and Development Journal for Engineering. 1(6).
- Kian, P. S. (2004). The use of outrigger and belt truss system for high-rise concrete buildings. Civil Engineering Dimension. 3(1), pp. 36-41.
- Kim, H.-S. (2017). "Optimum design of outriggers in a tall building by alternating nonlinear programming." Engineering Structures 150: 91-97.
- Kim, H.-S. (2018). "Optimum Locations of Outriggers in a Concrete Tall Building to Reduce Differential Axial Shortening." International Journal of Concrete Structures and Materials 12(1): 77.
- Kiran Kamath, Rao, S. and Shruthi (2015). Optimum Positioning of Outriggers to Reduce Differential Column Shortening Due to Long Term Effects in Tall Buildings. International Journal of Advanced Research in Science and Technology (IJARST). Volume 4(Issue 3), 353-357.
- KOMAL JAIN, J. M. G. S. K. (2016). An Analytical Study on Outrigger Structures Using Non Linear Dynamic Time History Analysis. International Research Journal of Engineering and Technology (IRJET). 03(04), 10.
- Krunal Z. Mistry, P. D. J. D. (2015). Optimum Outrigger Location in Outrigger Structural System for High Rise Building. International Journal of Advance Engineering and Research Development: IJAERD. 2(5).
- Kwangryang Chung, W. S. (2015). Outrigger Systems for Tall Buildings in Korea. International Journal of High-Rise Buildings. Vol 4(No 3), 9.
- Kwok, M. and Vesey, D. (1997). Reaching for the moon-A view on the future of tall buildings. Structures in the New Millennium, Lee (ed.), Balkema. 199-205.
- Lee, D., S. Shin and Q. H. Doan (2018). "Real-time robust assessment of angles and positions of nonscaled steel outrigger structure with Maxwell-Mohr method." Construction and Building Materials 186: 1161-1176.

- Lee, J., Bang, M. and Kim, J. Y. (2008). An analytical model for high-rise wall-frame structures with outriggers. *The Structural Design of Tall and Special Buildings*. 17(4), 839-851.
- Lee, S. and Tovar, A. (2014). Outrigger placement in tall buildings using topology optimization. *Engineering Structures*. 74, 122-129.
- Machado, F. (1965). The Messina earthquake of 1908 and the magma chamber of Etna. *Bulletin of Volcanology*. 28(1), 375-380.
- Manual, A. S. U. s. (2012). Abaqus 6.11.
- Marabi, B. and Marsono, A. K. (2016). A Numerical AND ANALYTICAL STUDY ON OPTIMISATION AND EFFICIENCY OF STRUCTURAL FORMS BY TWO-OUTRIGGER IN TALL BUILDINGS. *Malaysian Journal of Civil Engineering*. 3(28 Special Issue (3)), 17.
- Marshall Gerometta, C. (2009). Height: The History of Measuring Tall Buildings CTBUH (pp. World's Tallest Buildings).
- Mazzotta, V., E. Brunese and R. Nascimbene (2017). "Numerical Modeling and Seismic Analysis of Tall Steel Buildings with Braced Frame Systems." *Periodica Polytechnica Civil Engineering* 61(2): 196-208.
- Meek, J. L. (1971). Matrix structural analysis. McGraw-Hill Companies.
- Mirtalaei, K. and Zeidabadi, N. A. (2000). Parametric Study of Outrigger Braced and Belt System in Tall Building Structures.
- Mohamed, O. A. and O. Najm (2016). "Outrigger systems to mitigate disproportionate collapse in building structures." *Procedia engineering* 161: 839-844.
- Moinuddin, M. I. and Khan, M. (2010). Structural design of reinforced concrete tall buildings. *International Journal of Advanced Trends in Computer Science and Engineering*. 2(1), 628-633.
- Moon, K. S. (2011). "Outrigger Structures for Twisted Tall Buildings." *Advances in Civil Engineering*, Pts 1-6 255-260: 737-741.
- Nair, R. S. (1998). Belt trusses and basements as "virtual" outriggers for tall buildings. *ENGINEERING JOURNAL-AMERICAN INSTITUTE OF STEEL CONSTRUCTION*. 35, 140-146.
- Nanduri, P. R. K., Suresh, B. and Hussain, M. I. (2013). Optimum position of outrigger system for high-rise reinforced concrete buildings under wind and earthquake loadings. *American Journal of Engineering Research*. 2, 76-89.

- Neri, G., Barberi, G., Oliva, G. and Orecchio, B. (2004). Tectonic stress and seismogenic faulting in the area of the 1908 Messina earthquake, south Italy. *Geophysical research letters*. 31(10).
- Nie, J. and Ran, D. (2013). Experimental research on seismic performance of K-style steel outrigger truss to concrete core tube wall joints. *Proceedings of the 2013 ASCE Structures Congress*, 2802-2813.
- Rahgozar, R., Ahmadi, A. R. and Sharifi, Y. (2010). A simple mathematical model for approximate analysis of tall buildings. *Applied Mathematical Modelling*. 34(9), 2437-2451.
- Samat, R. A., Ali, N. M. and Marsono, A. K. (2008). The Optimum Location of Outrigger in Reducing the Along-Wind and Across-Wind Responses of Tall Buildings. *Malaysian Journal of Civil Engineering*. 20(2).
- Shahrooz, B. M., Deason, J. T. and Tunc, G. (2004a). Outrigger beam-wall connections. I: component testing and development of design model. *Journal of Structural Engineering*. 130(2), 253-261.
- Shahrooz, B. M., Tunc, G. and Deason, J. T. (2004b). Outrigger Beam-Wall Connections. II: Subassembly Testing and Further Modeling Enhancements. *Journal of Structural Engineering*. 130(2), 262-270.
- Shivacharan, K., Chandrakala, S. and Karthik, N. (2015a). Optimum Position of Outrigger System for Tall Vertical Irregularity Structures.
- Shivacharan, K., Chandrakala, S., Narayana, G. and Karthik, N. (2015b). Analysis of outrigger system for tall vertical irregularities structures subjected to lateral loads. *IJRET*.
- Simulia, D. (2010). *ABAQUS analysis user's manual*, version 6.10.
- Simulia, D. (2011). *ABAQUS 6.11 analysis user's manual*. Abaqus. 6, 22.22.
- Sinn, R., Bennetts, I. D. and Kilmister, M. B. (1995). *Structural systems for tall buildings*. McGraw-Hill Companies.
- Smith, B. S. (1980). Behavior of multi-outrigger braced tall building structures. *Special Publication*. 63, 515-542.
- Smith, B. S. and Coull, A. (1991). *Tall building structures: analysis and design*. University of Texas Press.
- Smith, B. S. and Coull, A. (1991). *Tall building structures: analysis and design*. University of Texas Press.

- Smith, B. S. and Salim, I. (1981). Parameter study of outrigger-braced tall building structures. *Journal of the Structural Division*. 107(10), 2001-2014.
- Smith, B. S. and Salim, I. (1983). Formulae for optimum drift resistance of outrigger braced tall building structures. *Computers & Structures*. 17(1), 45-50.
- Smith, R. and Willford, M. (2008). Damped outriggers for tall buildings. *The Arup Journal*. 3, 15-21.
- Srinivas Suresh Kogilgeri, B. S. (2015). A Study on Behaviour of Outrigger System on High Rise Steel Structure by Varying Outrigger Depth. *International Journal of Research in Engineering and Technology*. 04(07), 5.
- Standard, A. (2004a). E8-04, ". Standard Test Methods for Tension Testing of Metallic Materials," Annual Book of ASTM Standards. 3.
- Standard, A. (2004b). E8," Standard Test Methods for Tension Testing of Metallic Materials. Annual book of ASTM standards. 3, 57-72.
- Standard, B. (2005). Eurocode 8: Design of structures for earthquake resistance—.
- Takahashi, Y. and Fenves, G. L. (2006). Software framework for distributed experimental–computational simulation of structural systems. *Earthquake engineering & structural dynamics*. 35(3), 267-291.
- Tan, P., Fang, C., Tu, W., Zhou, F., Wang, Y. and Jiang, M. (2012). Experimental study on the outrigger damping system for high-rise building. *Proceedings of the 2012 Proceedings in the 15th World Conference on Earthquake Engineering, Lisbon, Portugal,*
- Taranath, B. (1998). *Steel, concrete, and composite design of tall buildings*. McGraw-Hill Professional.
- Taranath, B. S. (2004). *Wind and earthquake resistant buildings: Structural analysis and design*. CRC press.
- Taranath, B. S. (2009). *Reinforced concrete design of tall buildings*. CRC press.
- Taranath, B. S. (2011). *Structural analysis and design of tall buildings: Steel and composite construction*, CRC press.
- Thai, H.-T. and Kim, S.-E. (2009). Practical advanced analysis software for nonlinear inelastic analysis of space steel structures. *Advances in Engineering Software*. 40(9), 786-797.
- Vijaya Kumari Gowda M R, M. B. C. (2015). A Study on Dynamic Analysis of Tall Structure with Belt Truss Systems for Different Seismic Zones. *International Journal of Engineering Research & Technology (IJERT)*. 4(08).

- Wong, R. W. and Ho, M. Structural and Construction Feature of the Hong Kong International Financial Center Phase II.
- Wood, A. (2008). Best tall buildings 2008: CTBUH international award winning projects. Elsevier/Architectural Press.
- Wu, J. and Li, Q. (2003). Structural performance of multi-outrigger-braced tall buildings. The structural design of tall and special buildings. 12(2), 155-176.
- Wu, X. and Zhang, B. (2012). The Transformation of Nonlinear Structure Analysis Model From NosaCAD to ABAQUS and PERFORM-3D.
- Zeidabadi, N. A., Mirtalae, K. and Mobasher, B. (2004). Optimized use of the outrigger system to stiffen the coupled shear walls in tall buildings. The structural design of tall and special buildings. 13(1), 9-27.